Numerical Simulations of the Effects of Microstructure on Photonic Crystals

by

Martin Maldovan

Submitted to the Department of Materials Science and Engineering

in partial fulfillment of the requirements for the degree of

Master of Science in Materials Science

at the

MASSACHUSETTS INSTITUTE OF TECHNOLOGY

February, 2001

Author _____
Department of Materials Science and Engineering
Jan 19, 2001

Certified by _____
W. Craig Carter
Thomas Lord Associate Professor of Materials Science and Engineering
Thesis Supervisor

Accepted by _____
Harry L. Tuller
Professor of Ceramics and Electronic Materials
Chair, Departmental Committee on Graduate Students

Numerical Simulations of the Effects of Microstructure on Photonic Crystals

by

Martin Maldovan

Submitted to the Department of Materials Science and Engineering on Jan 19, 2001,

in partial fulfillment of the requirements for the degree of

Master of Science in Materials Science

Abstract

The optical properties of photonic crystals were studied to gain an understanding of the response of these structures to electromagnetic waves. In particular, multilayer films and two-dimensional systems were studied. It is known that multilayer films present omnidirectional reflectivity for a certain range of frequencies. A numerical technique for solving the Maxwell's equations within infinite periodic structures is presented. The media are assumed to be isotropic, linear, and non-conducting. This technique is based on the Fourier Transform of the dielectric constant of the structure. The numerical formulation allows the determination of the dispersion curves for photonic crystals. From them, omnidirectional reflectivity can be studied. The formulation was used to find the range of forbidden frequencies within an infinite multilayer film composed of two alternating materials. The energy gap for several constitutive parameters is shown. A two-dimensional system composed of infinite rods in a square lattice was also treated with this method. The Matrix Translation Method for studying omnidirectional reflectivity in one-dimensional systems was also used. This method considers homogeneous media and the electromagnetic fields are matched at the interfaces between the media. The formulation is used to obtain the reflectivity of the multilayer film as a function of the direction and frequency of the incident wave. By taking into account all directions and frequencies, omnidirectionality can be found. The method was applied to a finite multilayer film and the results are compared to those obtained with the Fast Fourier Transform Method. Similar results were obtained.
An understanding of the properties of photonic crystals was achieved and guidelines for the determination of energy gaps are presented.

Thesis Supervisor: W. Craig Carter
Title: Thomas Lord Associate Professor of Materials Science and Engineering

Contents

List of figures

Acknowledgments

I would like to thank my advisor Professor W.C. Carter, for his generous advice and support in this project and other areas.

I would like to thank my friends and colleagues Chaitanya Ullal and Miguel Marioni for sharing everything.

I would like to thank Singapore –MIT Alliance for their financial support.

I would like to thank my family for their love and understanding.

Finally, I would like to thank my brother Juan Pablo Maldovan.

Chapter 1

Introduction

1.1 Background

Electromagnetic wave propagation has been studied for many years.[1-2] However, in recent years this subject has been of heightened interest because of the conception and development of a group of materials that are now known as "photonic band gap materials" (PBG materials).[3-4]

The concept of photonic band gap materials was developed in analogy to the behavior electrons in semiconductors. The fact that electrons in semiconducting materials cannot possess certain energies permits the creation of many useful materials for device applications. A gap exists in the continuum of allowable electron energies. In other words, an electron possessing energy that places it within the "electronic" gap cannot travel within the medium. [5-6] This phenomenon is mainly attributed to the interaction of the electron with the periodic potential of the lattice whereby the atoms in the lattice act as centers of dispersion for the wave function of the electron. This idea of periodicity giving rise to a forbidden range of energies was exported to the propagation of electromagnetic radiation within materials. Recognizing that the corresponding periodic atomic potential for light is a periodically varying dielectric constant makes the analogy of a band gap for photons in the place of electrons.

Initial studies of PBG materials focused on three-dimensional photonic crystals and the attempt to prove the existence of the photonic band gaps.[7-8-9] The studies were subsequently applied to one- and two-dimensional systems. In the case of 1-D systems, multilayer systems composed of nine alternating layers with different dielectric constants were shown to have an omnidirectional gap.[10] In these systems, light with frequencies in the photonic gap could not exist within the crystal for any incident direction. A "perfect mirror" was thus created.

The study of configurations containing band gaps has been accompanied by the development of techniques for modeling this behavior. The objects of this modeling are, among other things, the development of band diagrams and the visualization of the flow of light in these media. To obtain the desired results, Maxwell's equations must be solved with boundary conditions that mimic those of PBG microstructures. One of the methods utilized to solve them was the assumption of an infinitely periodic structure. Periodic boundary conditions could be applied and the plane wave method was introduced. Central to this method is the transformation of the dielectric constant from real to reciprocal space via the Fourier Transform.[11]

The goal of this thesis project is to understand and demonstrate the application of the plane wave method for photonic crystals. This was done in the following manner:

1) The governing differential equation was obtained for the types of materials considered. The plane wave method was then applied to reduce the differential equation to an eigenvalue problem.
2) The method was applied to one- and two-dimensional systems using a FORTRAN code developed to solve the eigenvalue problem. Allowed and forbidden frequencies could be obtained.
3) Dispersion curves, band gaps, and color maps were evaluated for given photonic crystals and compared to data from the literature.
4) Finally, an optional method for studying omnidirectional frequency gaps in one-dimensional systems was presented. This method is called the Matrix Translation

Method. Results obtained with this formulation were compared to those obtained with the plane wave method.

1.2 Organization of the thesis

Chapter 2 presents the mathematical formulation for treating infinite periodic structures. The media are considered be isotropic, linear, and non-conducting. The governing differential equation is obtained from Maxwell's equations. The dielectric constant of the photonic crystal is transformed from real space to reciprocal space by using the Fast Fourier Transform method. This permits calculation of dispersion curves for the structure, the allowed, and the forbidden frequencies. By using this methodology, the energy gaps for infinite periodic structures can be obtained.

In Chapter 3 the above method is used and applied to a multilayer film. The structure consists of alternating layers characterized by its thickness and dielectric constant. Dispersion curves relating the frequency ω of the traveling wave to its wave vector $\mathbf{k}$ are found. First, planes waves that are normal to the multilayer interfaces are considered. Allowed and forbidden traveling frequencies are obtained for a multilayer film consisting of periodic bilayers characterized by the lengths and dielectric constants h_1=0.8μm, h_2= μm, ε_1=21.16, ε_2=2.56. For this structure, an omnidirectional gap is predicted numerically. Finally, graphs showing the normalized frequencies for the first energy gap for normal incident plane waves are included.

In Chapter 4 Fourier's method is applied to a two-dimensional system. A square lattice of dielectric columns is studied. The dispersion curves for this structure are obtained but no complete photonic band gap is found. However, a gap for transverse electric polarization is predicted. Color maps illustrating the spatial distribution of field intensity inside the photonic crystals are shown. An energy analysis can be done from the distribution of intensities.

Chapter 5 presents the Matrix Translation Method to obtain reflectivity for a multilayer film of finite dimension. The media forming the structure is considered to be isotropic, linear, homogeneous, and non-conducting. Matching conditions for the electromagnetic fields on the surfaces of the media allows the relationships between the fields in adjacent layers to be determined. These relations can be expressed in matrix notation. By translating the relationships from the first surface to the last surface of the multilayer film, reflectivity can be found. This methodology is used to find reflectivity for finite multilayer films. By considering all directions and frequencies for the incident wave, omnidirectionality can also be studied with this method. Reflectivity for a finite multilayer film composed of 14 layers is numerically determined. The parameters for the layers used in Chapter 3 are again considered in this case. The results show an excellent agreement with those for infinite media found with the Fourier's Method and provide insight into the convergence of finite multilayer films to the infinite limit.

Chapter 6 presents the conclusions for this work and suggestions for additional research.

Chapter 2

Fourier's Method:

Mathematical formulation

Each electromagnetic process is governed by the set of Maxwell's equations together with the constitutive relationships for the media through which electromagnetic energy is being propagated and the interface conditions. The phenomena of propagation inside a photonic crystal are likewise described by Maxwell's equations. But the solution of the Maxwell's equations is convoluted because the geometric and spatial distribution of the material constituents is complex. A numerical method for treating the Maxwell's equations in order to obtain the response of a photonic crystal during the propagation of an electromagnetic wave is treated in this chapter. The crystal will be considered to be composed of differing constituents *isotropic, linear, and nonconducting media.* This method is based on the translational symmetry of the photonic crystal. The dielectric constant of the structure is transformed using the Fast Fourier Transform scheme. By doing this, the problem is reduced to a standard eigenvalue problem.

2.1 Maxwell's equations

The basic laws of electricity and magnetism can be transformed into four mathematical expressions that form the set of Maxwell's equations

$$\nabla \times \mathbf{E}(\mathbf{r},t) + \frac{\partial \mathbf{B}(\mathbf{r},t)}{\partial t} = 0 \tag{2-1}$$

$$\nabla \times \mathbf{H}(\mathbf{r},t) - \frac{\partial \mathbf{D}(\mathbf{r},t)}{\partial t} = \mathbf{J}(\mathbf{r},t) \tag{2-2}$$

$$\nabla \cdot \mathbf{B}(\mathbf{r},t) = 0 \tag{2-3}$$

$$\nabla \cdot \mathbf{D}(\mathbf{r},t) = \rho(\mathbf{r},t) \tag{2-4}$$

Where

$\mathbf{E}(\mathbf{r},t)$ = Electric field intensity vector

$\mathbf{H}(\mathbf{r},t)$ = Magnetic field intensity vector

$\mathbf{D}(\mathbf{r},t)$ = Electric displacement vector

$\mathbf{B}(\mathbf{r},t)$ = Magnetic induction vector

$\mathbf{J}(\mathbf{r},t)$ = Current density vector

$\rho(\mathbf{r},t)$ = Density of charge

$\mathbf{r}$ = Position vector

t = Time

In turn $\mathbf{D}(\mathbf{r},t)$ and $\mathbf{H}(\mathbf{r},t)$ are related respectively to $\mathbf{E}(\mathbf{r},t)$ and $\mathbf{B}(\mathbf{r},t)$ by constitutive parameters that characterize the electromagnetic nature of the material medium involved. For an isotropic linear nonconducting medium the constitutive relations are

$$\mathbf{D}(\mathbf{r},t) = \varepsilon(\mathbf{r})\,\mathbf{E}(\mathbf{r},t) \tag{2-5}$$

$$\mathbf{B}(\mathbf{r},t) = \mu(\mathbf{r})\,\mathbf{H}(\mathbf{r},t) \tag{2-6}$$

where the constitutive parameters $\varepsilon(\mathbf{r})$ and $\mu(\mathbf{r})$ are respectively the dielectric constant and the permeability of the medium. In these types of media, Maxwell's equations reduce to

$$\nabla \times \mathbf{E}(\mathbf{r},t) + \mu(\mathbf{r}) \frac{\partial \mathbf{H}(\mathbf{r},t)}{\partial t} = 0 \tag{2-7}$$

$$\nabla \times \mathbf{H}(\mathbf{r},t) - \varepsilon(\mathbf{r}) \frac{\partial \mathbf{E}(\mathbf{r},t)}{\partial t} = \mathbf{J}(\mathbf{r},t) \tag{2-8}$$

$$\nabla \cdot \mu(\mathbf{r}) \mathbf{H}(\mathbf{r},t) = 0 \tag{2-9}$$

$$\nabla \cdot \varepsilon(\mathbf{r}) \mathbf{E}(\mathbf{r},t) = \rho(\mathbf{r},t) \tag{2-10}$$

Taking the curl of Eq. (2-8) and considering Eq. (2-7) leads to

$$\nabla \times \left(\frac{1}{\varepsilon(\mathbf{r})} \nabla \times \mathbf{H}(\mathbf{r},t) \right) + \mu(\mathbf{r}) \frac{\partial^2 \mathbf{H}(\mathbf{r},t)}{\partial t^2} = \nabla \times \left(\frac{1}{\varepsilon(\mathbf{r})} \mathbf{J}(\mathbf{r},t) \right) \tag{2-11}$$

The wave vector equation (2-11) serves to determine $\mathbf{H}(\mathbf{r},t)$ at each point and any time within the photonic crystal characterized by $\varepsilon(\mathbf{r})$ and $\mu(\mathbf{r})$. Propagation within several adjoining dielectric media with no currents (neither source currents nor induced currents) will be considered, then the *fundamental* equation to be solved becomes

$$\nabla \times \left(\frac{1}{\varepsilon(\mathbf{r})} \nabla \times \mathbf{H}(\mathbf{r},t) \right) + \mu(\mathbf{r}) \frac{\partial^2 \mathbf{H}(\mathbf{r},t)}{\partial t^2} = 0 \tag{2-12}$$

2.2 Time dependence

Because Maxwell's equations form a linear system, considering the "monochromatic" state, in which all quantities are simply periodic in time, because any other solution can be obtained by superposition of monochromatic solutions, loses no generality. Each monochromatic solution will be referred to as a "magnetic mode." Then, the following convention for the time dependence is chosen

(2-13)

$$\mathbf{H}(\mathbf{r},t) = \mathrm{Re}\{\mathbf{H}_\omega(\mathbf{r})\, e^{i\omega t}\}$$

Substituting into the fundamental equation (2-12) yields

$$\nabla\times\left(\frac{1}{\varepsilon(\mathbf{r})}\nabla\times\mathbf{H}_\omega(\mathbf{r})\right)-\mu(\mathbf{r})\omega^2\mathbf{H}_\omega(\mathbf{r})=0$$

Reordering terms and taking into account that

$$\varepsilon_r(\mathbf{r})=\frac{\varepsilon(\mathbf{r})}{\varepsilon_0}\qquad \mu_r(\mathbf{r})=\frac{\mu(\mathbf{r})}{\mu_0}\qquad c=\frac{1}{\sqrt{\varepsilon_0\mu_0}} \tag{2-15}$$

where $\varepsilon_0 = 8.854\,10^{-12}\ F/m$, $\mu_0 = 4\cdot\pi\ 10^{-7}\ H/m$, and c is the speed of the light, we obtain the final *fundamental* equation for the spatial dependence of the magnetic field $\mathbf{H}_\omega(\mathbf{r})$

$$\nabla\times\left(\frac{1}{\varepsilon_r(\mathbf{r})}\nabla\times\mathbf{H}_\omega(\mathbf{r})\right)=\mu_r(\mathbf{r})\frac{\omega^2}{c^2}\mathbf{H}_\omega(\mathbf{r}) \tag{2-16}$$

The aim is to solve this fundamental equation for a given photonic crystal with a geometry characterized by $\varepsilon(\mathbf{r})$ and $\mu(\mathbf{r})$. This equation will indicate which magnetic modes are allowed to travel within the crystal and their associated wave vector. It will also indicate the modes for which no traveling wave is allowed inside the photonic crystal (i.e. a frequency corresponding to a photon within the photonic band gap). All such energies and wavevectors comprise a photonic band diagram.

2.3 Spatial dependence

Because of the periodicity of photonic crystals, the dielectric constant $\varepsilon_r(\mathbf{r})$ and the magnetic field $\mathbf{H}_\omega(\mathbf{r})$ can be expanded in series as demonstrated in the the following sections.

2.3.1 The dielectric constant $\varepsilon_r(\mathbf{r})$

Crystals for which $\mu_r(\mathbf{r}) = 1$ throughout all the space are studied. All the information about our photonic crystal or any other dielectric configuration is given by $\varepsilon_r(\mathbf{r})$. In the case of a photonic crystal certain periodicity is satisfied, then

$$\varepsilon(\mathbf{r}) = \varepsilon(\mathbf{r} + \mathbf{R}) \tag{2-17}$$

with $\mathbf{R}=l\mathbf{a}+ m\mathbf{b} +n\mathbf{c}$ where (l, m, n) are integers and ($\mathbf{a}$, $\mathbf{b}$, $\mathbf{c}$) are the primitive lattice vectors. Because of this translational symmetry $\varepsilon_r(\mathbf{r})$ can be expanded in the following way

$$\varepsilon(\mathbf{r}) = \sum_{\mathbf{G}} \varepsilon_{\mathbf{G}}\, e^{i\mathbf{G}\cdot\mathbf{r}} \tag{2-18}$$

with $\mathbf{G}=l\mathbf{b}_1+ m\mathbf{b}_2 +n\mathbf{b}_3$ where (l, m, n) are integers and ($\mathbf{b}_1$, $\mathbf{b}_2$, $\mathbf{b}_3$) are the reciprocal lattice vectors.

2.3.2 The magnetic field $\mathbf{H}_\omega(\mathbf{r})$

The fundamental equation (2-16) can be written as an eigenvalue equation

$$\hat{\mathrm{A}}\,\mathbf{H}_\omega(\mathbf{r}) = a\,\mathbf{H}_\omega(\mathbf{r}) \tag{2-19}$$

where $\hat{\mathrm{A}}$ is the operator $\nabla\times\left(\frac{1}{\varepsilon_r(\mathbf{r})}\nabla\times\right)$ and $a = \frac{\omega^2}{c^2}$. Since $\varepsilon(\mathbf{r})$ is periodic we can expand the solution for each component of $\mathbf{H}_\omega(\mathbf{r})$ using Bloch's theorem.[6]

$$\mathrm{H}_\omega^{\mathbf{k}}(\mathbf{r}) = e^{i\mathbf{k}\cdot\mathbf{r}}\, u_\omega^{\mathbf{k}}(\mathbf{r}) \tag{2-20}$$

where $u_{\omega}^{\mathbf{k}}(\mathbf{r}+\mathbf{R}) = u_{\omega}^{\mathbf{k}}(\mathbf{r})$ and **k** is a wave vector in the Brillouin zone of the lattice. Because the function *u* has translational symmetry

$$\mathbf{H}_{\omega}^{\mathbf{k}}(\mathbf{r}) = \sum_{\mathbf{G}} \sum_{\lambda=1}^{2} h_{\mathbf{G},\lambda} \hat{e}_{\lambda} e^{i(\mathbf{k}+\mathbf{G})\cdot\mathbf{r}} \tag{2-21}$$

where $\hat{e}_1, \hat{e}_2$ are unit vectors orthogonal to **k**+**G** because $\mathbf{H}_{\omega}^{\mathbf{k}}(\mathbf{r})$ obeys Maxwell's equation $\nabla \cdot \mathbf{H}_{\omega}^{\mathbf{k}}(\mathbf{r}) = 0$.

2.4 Solving the fundamental equation

Inserting the spatial expansions for the dielectric constant and magnetic field into the fundamental equation leads to the following system of linear equations.[12]

$$\sum_{(\mathbf{G},\lambda)'} \left[(\mathbf{k}+\mathbf{G}) \times \hat{e}_{\lambda} \right] \cdot \left[(\mathbf{k}+\mathbf{G}') \times \hat{e}_{\lambda'} \right] \varepsilon^{-1}(\mathbf{G},\mathbf{G}') \, h_{\mathbf{G},\lambda} = \left(\frac{\omega}{c} \right)^2 h_{\mathbf{G},\lambda} \tag{2-22}$$

where the unknown $h_{\mathbf{G},\lambda}$ are the expansion coefficients for **H**.

In this equation $\varepsilon^{-1}(\mathbf{G},\mathbf{G}')$ is the inverse of the Fourier Transform of the dielectric function $\varepsilon_r(\mathbf{r})$. In order to obtain these coefficients numerically, an efficient computational scheme called Fast Fourier Transform (FFT) is used. It transforms the dielectric function from real space $\varepsilon_r(\mathbf{r})$ to reciprocal space.

This is a standard eigenvalue problem. The procedure to solve the problem is the following: for a given value of **k** in the Brillouin zone, the matrix on the left-hand of Eq. (2-22) is constructed. Once the eigenvalue problem is solved numerically, all frequencies ω corresponding to that particular value of **k** are obtained. By repeating the process for *all* the values of **k** in the Brillouin zone, plots of $\omega(\mathbf{k})$ for each band can be drawn. This is the final result: the band structure for a particular photonic crystal.

2.5 Scaling properties

The fundamental equation (2-16) permits the following scaling properties. There is no fundamental length in the studying of photonic crystals. If the solution for a given spatial scale is known, the solution for a compression or expansion of the spatial configuration can be simply obtained by scaling a solution determined for a given length scale. Furthermore, there is no fundamental value for the dielectric constant. If the solution for a given dielectric configuration is known, the solution for a new configuration, in which the dielectric constant differs in all corresponding spatial regions by a constant factor, can be also simply obtained by scaling a known solution.

2.5.1 Spatial scaling

Recalling the fundamental equation (2-16) with $\mu_r=1$

$$\nabla\times\left(\frac{1}{\varepsilon_r(\mathbf{r})}\nabla\times\mathbf{H}_\omega(\mathbf{r})\right)=\frac{\omega^2}{c^2}\mathbf{H}_\omega(\mathbf{r}) \tag{2-23}$$

it is possible to make the following change of variables $\mathbf{r}'=s\mathbf{r}$ and $\nabla'=\nabla/s$ and obtain

$$\nabla'\times\left(\frac{1}{\varepsilon_r(\mathbf{r}'/s)}\nabla'\times\mathbf{H}_{\omega'}(\mathbf{r}'/s)\right)=\frac{\omega^2}{(cs)^2}\mathbf{H}_{\omega'}(\mathbf{r}'/s) \tag{2-24}$$

By comparing Eq. (2-23) and (2-24) the following scaling relations arise. Assume that the mode $\mathbf{H}_\omega(\mathbf{r})$ with frequency ω represents the solution for the dielectric configuration $\varepsilon_r(\mathbf{r})$. If the dielectric configuration is compressed or expanded by a factor s, the new solution mode will be the scaled old mode $\mathbf{H}_{\omega'}(\mathbf{r}'/s)$ having a scaled frequency $\omega'=\omega/s$. The solution of the problem at one scale determines the solution of the problem at all other length scales.

2.5.2 Scaling the dielectric constant

Recalling Eq. (2-16)

$$\nabla\times\left(\frac{1}{\varepsilon_r(\mathbf{r})}\nabla\times\mathbf{H}_\omega(\mathbf{r})\right)=\frac{\omega^2}{c^2}\mathbf{H}_\omega(\mathbf{r}) \tag{2-25}$$

and making the change $\varepsilon'_r(\mathbf{r})= \varepsilon_r(\mathbf{r})/s^2$ the following equation is obtained

$$\nabla\times\left(\frac{1}{\varepsilon'_r(\mathbf{r})}\nabla\times\mathbf{H}_\omega(\mathbf{r})\right)=\frac{(s\,\omega)^2}{c^2}\mathbf{H}_\omega(\mathbf{r}) \tag{2-26}$$

By comparing (2-25) and (2-26) it can be seen that the modes for the new dielectric configuration are the same. If the solution for a given dielectric configuration is known, the solution for the configuration in which the dielectric constant differs in a factor is the same but the frequency must be scaled. The new frequency is the old frequency multiplied by *s*. The solution of the problem for a dielectric configuration determines the solution for the other dielectric configurations for which the difference is just a constant factor.

Chapter 3

Fourier's Method:

Band diagrams for 1-D photonic crystals

Using the formulation described in the last chapter, band diagrams for a given photonic crystal characterized by the dielectric constant $\varepsilon(\mathbf{r})$ are obtained. In this chapter, the formulation is applied to a one-dimensional photonic crystal (Fig. 3-1) composed of alternating layers of widths h_1 and h_2 and dielectric constants ε_1, ε_2 respectively.

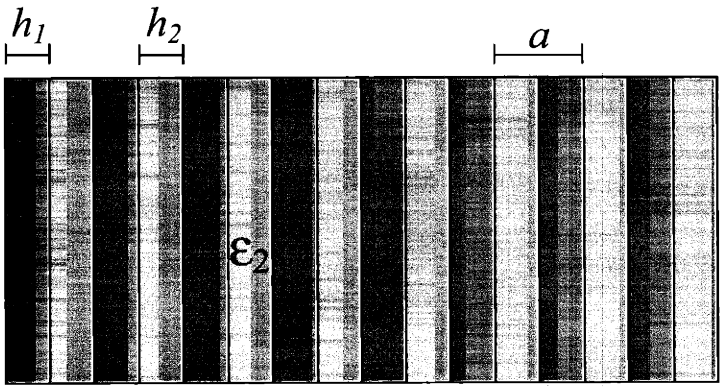

Fig. 3-1 One dimensional photonic crystal formed by alternating layers of different dielectric constants and thickness.

3.1 Transverse electric and transverse magnetic modes

The response of the photonic crystal to an electromagnetic excitation depends strongly on the polarization of the wave. Because electromagnetic waves are transversal waves, the magnetic field **H** resides in a plane perpendicular to the direction of propagation of the wave. In the plane two unit vectors are chosen by convention. Each general magnetic field **H** can be decomposed in these two directions. One is called transverse electric (TE) and the other transverse magnetic (TM). The following figures describe the convention.

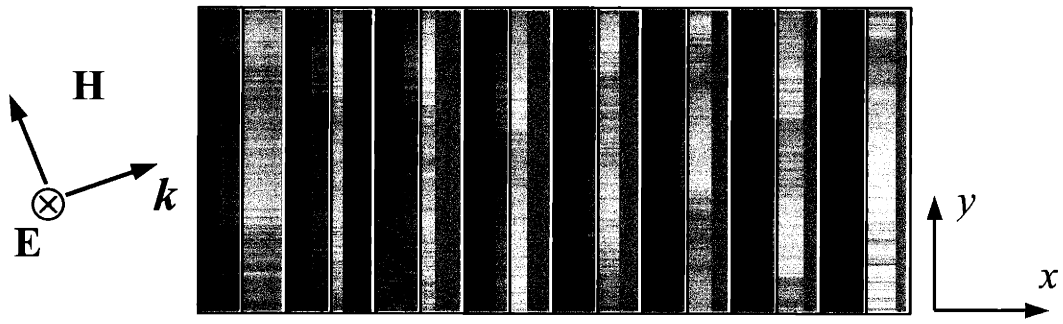

Fig. 3-2 Transverse electric mode. **H** perpendicular to the wave vector **k**. Both in the plane of the sheet.

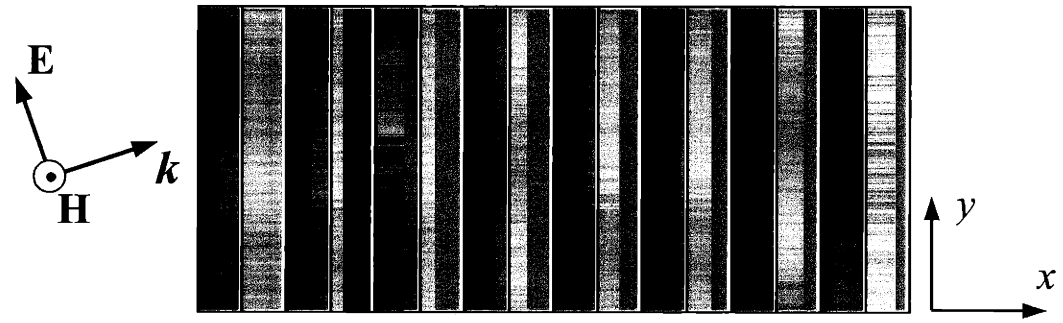

Fig. 3-3 Transverse magnetic mode. **H** perpendicular to the wave vector **k** and the plane of the sheet.

3.2 Band diagram for perpendicular incidence

The response of the photonic crystal to a perpendicular incident electromagnetic wave is obtained. Because of symmetry in this case there is no difference between the transverse and the magnetic modes. The values for the thickness h_1, h_2, and the dielectric constants ε_1, ε_2, are chosen in order to reproduce the results in Fink et al.[10] as a check on the numerical algorithm that was developed as part of this thesis. The values for the layers are h_1=0.8μm, h_2=1.65μm and ε_1=21.16, ε_2=2.56 respectively. When the incident wave is perpendicular to the layers the angle of incidence is zero therefore the only remaining variable is the modulus of the wave vector **k**.

The values of **k** over the entire Brillouin zone are mapped because all the information is obtained from this zone due to the symmetry of the crystal in the x direction. For each value of **k** the correspondent frequencies (eigenvalues of the fundamental equation) are found and all the results are plotted in the same graph. By doing this, the band diagram for perpendicular incidence is obtained.

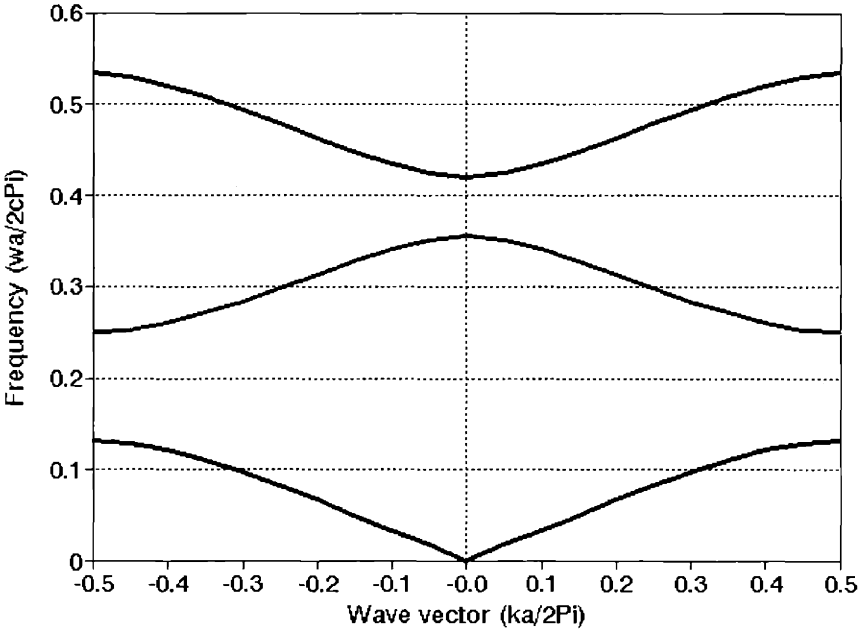

Fig. 3-4 Band diagram for perpendicular incidence. The photonic crystal is characterized by h_1=0.8μm h_2=1.65μm a=2.45μm ε_1=21.16 ε_2=2.56. The first three bands are shown.

The following data can be obtained from the figure. First, the dispersion relationship $\omega(\mathbf{k})$ can be determined as a function of the wave vector **k**. Also, it can be seen from the figure that all frequencies are not allowed to travel inside the photonic crystal in the (100) direction. The figure also shows the frequencies that are forbidden. By plotting three bands, two complete gaps of frequencies can be seen.

The range of both allowed and forbidden frequencies for each examined direction is taken as the final result. All the values of the component of the wave vector **k** in the x direction within the Brillouin zone are plotted. Finally, by projecting the bands on the central axis, allowed and forbidden frequencies for that particular direction are found. A visual representation of the result is illustrated by the following figure.

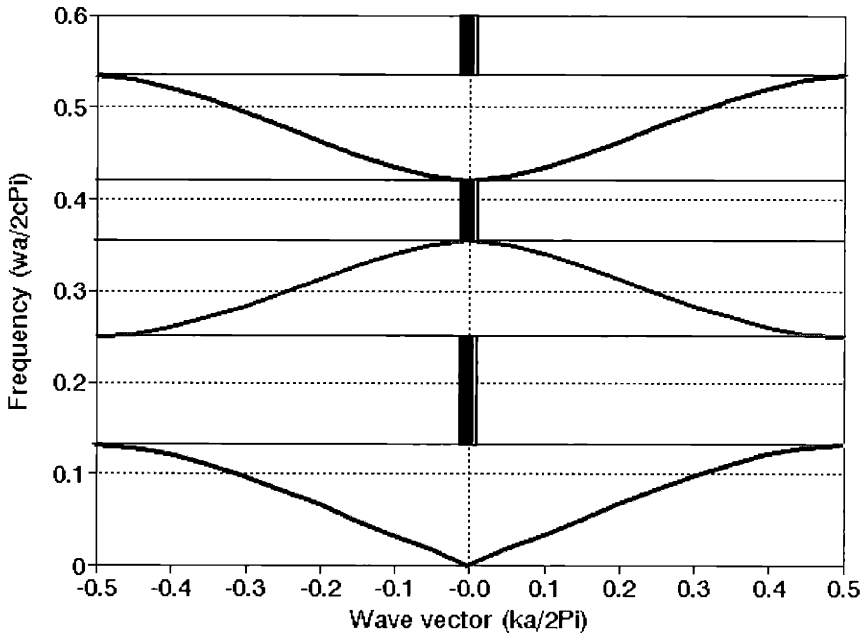

Fig. 3-5 Forbidden frequencies (orange). These ranges are the result extracted from the graph for a particular direction, in this case (100).

The results indicate that the first gap is comprised of those frequencies for which $\frac{\omega a}{2c\pi}$ fall into the range 0.1317-0.2497 and a second gap for the range 0.3548-0.4192.

3.3 Band diagram for all directions

The treatment of all incident directions for the electromagnetic wave is now considered. The results can be arranged as follows. Because the photonic crystal has translational symmetry in the x direction, only values of k_x within the Brillouin zone are needed. The same cannot be applied to the y direction because in this direction there is no translational symmetry. In this case, the advantage of having all the information within a zone is lost. Therefore k_y can take any value.

The allowed and forbidden frequencies obtained for all directions are projected on the ω-k_y plane. The directions are labeled by k_y and it is implicit that the values of k_x are those in the Brillouin zone.

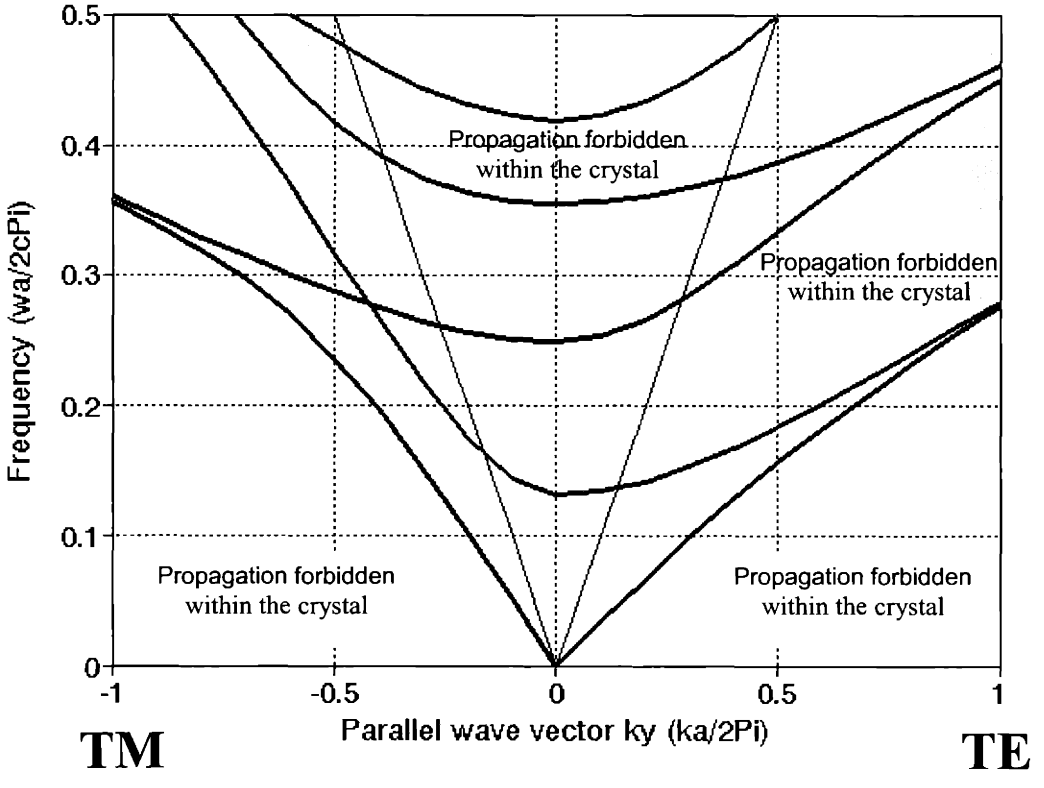

Fig. 3-6 Projected band diagram for a one dimensional photonic crystal composed of alternating layers with thickness h_1=0.8μm, h_2=1.65μm and dielectric constants ε_1=21.16, ε_2=2.56. Allowed states for external light incident on the photonic crystal are represented for the interior area of the light cone. The structure presents an omnidirectional gap.

The case k_y=0 corresponds to the previous example in which the direction of propagation was perpendicular to the layers. The forbidden ranges in the central axis of Fig. 3-6 correspond to the orange forbidden ranges in Fig. 3-5.

An interesting phenomenon is the dependence of the photonic properties on the angle of incidence of the plane wave with respect to the interface normal. The allowed states for this external light are those falling inside of the light cone shown in the figure. If one wants to know if light incident from the exterior is allowed to propagate inside the crystal, one need consider only those results within the light cone.

Considering only this part of the graph, it is important to highlight the existence of a range of frequencies for which propagation is forbidden for all directions. It is important to note that, for the dielectric constants used in this case, the Brewster line falls outside of the light cone. As a result, the structure presents an omnidirectional gap and the photonic crystal behaves as a perfect mirror.

3.4 Normalized first energy gap for normal incidence

By considering the scaling properties mentioned in Chapter 2, the following graphs for the first energy gap for normal incidence can be obtained. Because there is no fundamental length and dielectric value, the forbidden frequencies for a scaled solution can be obtained from the forbidden frequencies for an unscaled solution. These graphs can be used to determine the first energy gaps for a doubly infinite set of photonic crystal configurations.

The following two graphs (Fig. 3-7 and Fig. 3-8) show the upper and lower normalized values of the first energy gap (normal incidence). The values are plotted as a function of the volume fraction of medium one in the configuration and for different values of n_2/ n_1. In Fig. 3-9, the middle value for the energy gap can be seen. Fig. 3-10 shows the width of the energy gap. These forbidden frequency values represent the first energy gap for normal incidence. The values differ from the results obtained for omnidirectional reflectivity.

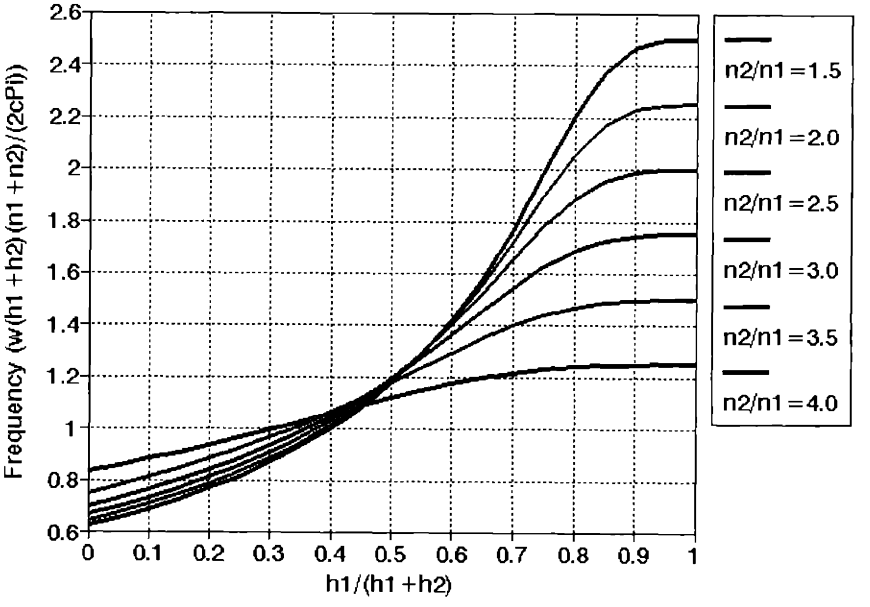

Fig. 3-7 Normalized top values for the first energy gap (normal incidence).

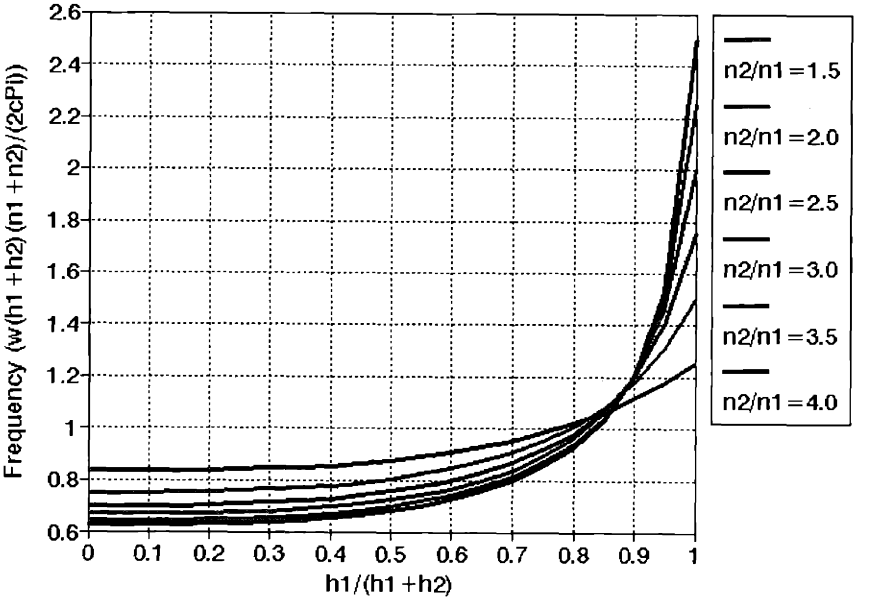

Fig. 3-8 Normalized bottom values for the first energy gap (normal incidence).

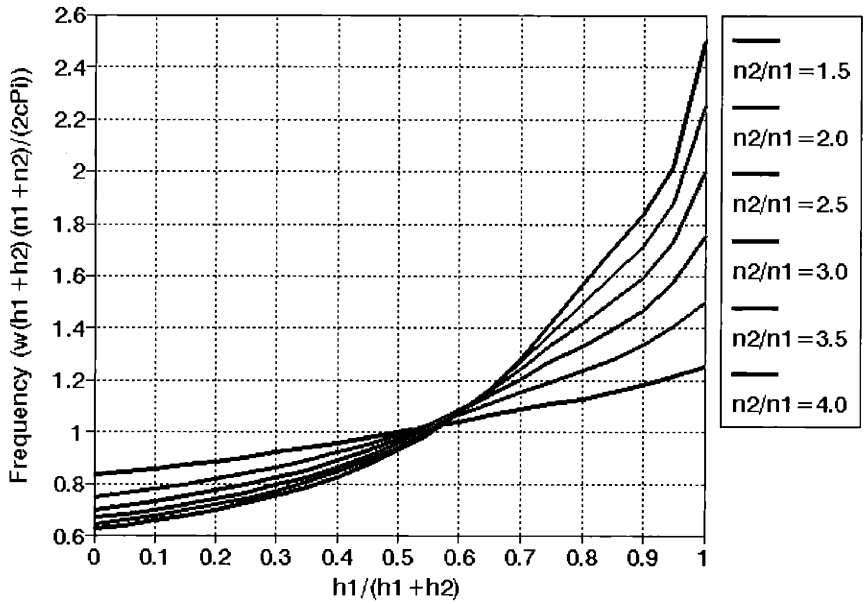

Fig. 3-9 Normalized middle values for the first energy gap (normal incidence).

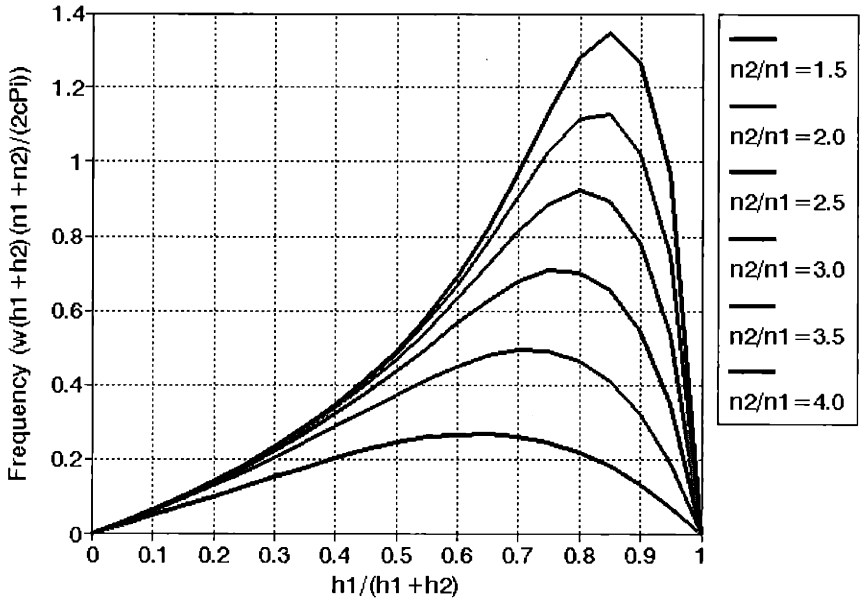

Fig. 3-10 Normalized width values for the first energy gap (normal incidence).

Chapter 4

Fourier's Method:

Band diagrams for 2-D photonic crystals

In this chapter Fourier's Method is extended to infinite two-dimensional systems. In particular, a square lattice of dielectric columns is studied (Fig. 4-1). The x-y transversal plane to the dielectric cylinders is shown in the figure and it is assumed that the columns are infinite along the longitudinal direction z. Waves propagating in the transversal plane are considered to be the only other mode. In other words, the wave vector has components only in the x and y directions. These types of lattices are defined by the dielectric constants of the materials that form the photonic crystal and the quotient between the radius of the cylinders r and the lattice constant a. The square array of dielectric columns has a square reciprocal lattice. As a result, the Brillouin zone for the structure is also square.

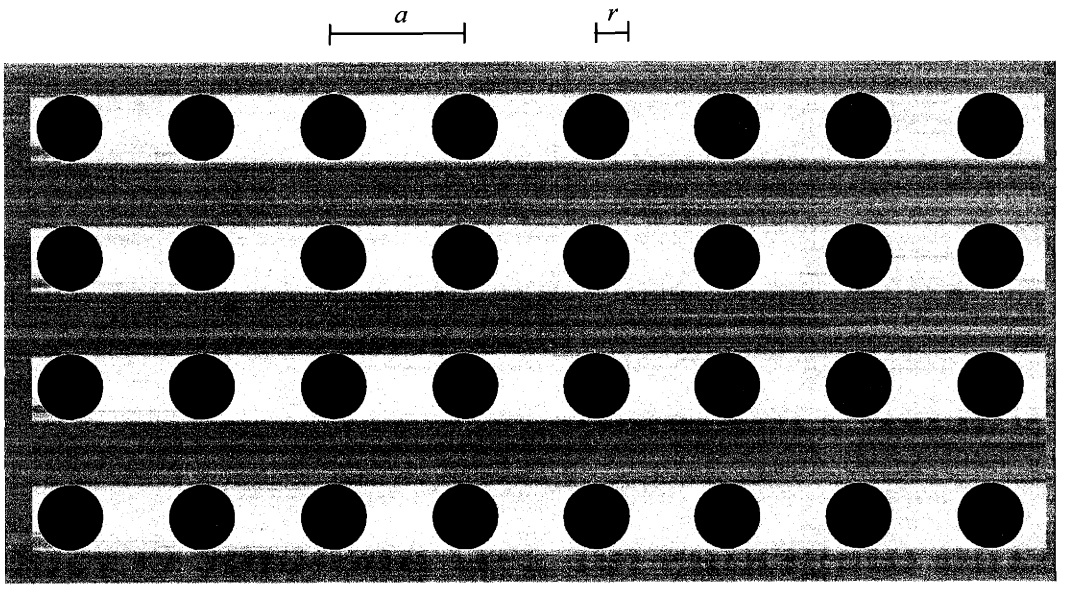

Fig. 4-1 Two-dimensional photonic crystal. The structure consists of a square array of dielectric cylinders with radius r in a lattice with constant a.

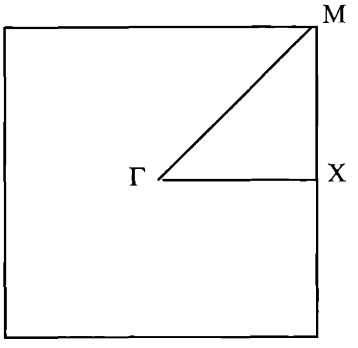

Fig. 4-2 Brillouin zone and irreducible Brillouin zone (triangle) for the square array of dielectric cylinders.

4.1 Band diagrams for a square lattice of dielectric cylinders

The irreducible Brillouin zone is shown in Fig. 4-2 (triangle). All other points in the Brillouin zone can be related to a point in the irreducible Brillouin zone through rotational

transformations. The standard band diagram for this type of structure shows the results along the edges of the triangular zone. The band structure is calculated for a photonic crystal consisting of cylinders with r=0.2 a. The value for the dielectric constant of the column is assumed to have a value ε=8.9 and the matrix (air) has a dielectric constant ε=1. Diagrams for transverse electric and transverse magnetic polarization are shown separately.

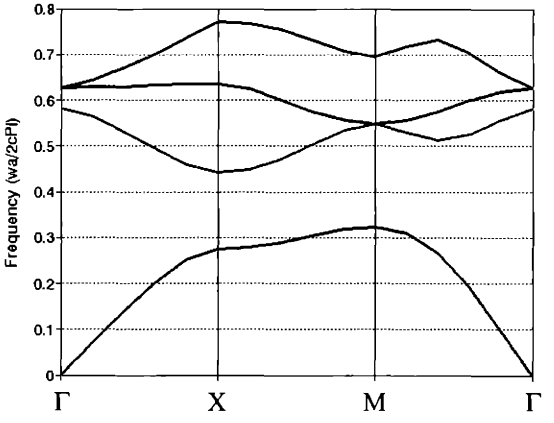

Fig. 4-3 Band structure for a square lattice of dielectric columns (TE polarization). The dielectric constants are ε=8.9 for the cylinders and ε=1 for the matrix.

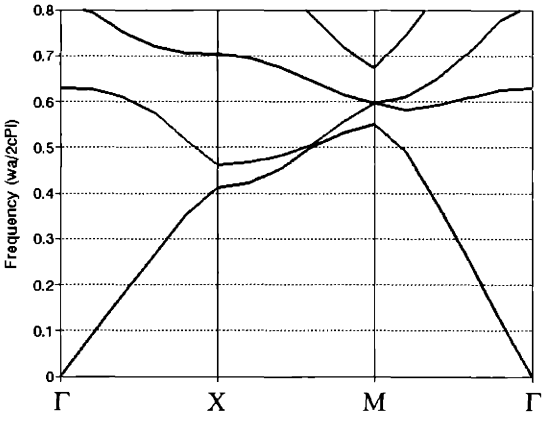

Fig. 4-4 Band structure for a square lattice of dielectric columns (TM polarization). The dielectric constants are ε=8.9 for the cylinders and ε=1 for the matrix.

From Figs. 4-3 and 4-4, it can be seen that there is no gap for transverse magnetic polarization but a photonic band gap exists for transverse electric polarization.

4.2 Color maps for the distributions of the fields

As a final result for two-dimensional systems, color maps are obtained for specific points on the edges of the irreducible Brillouin zone. For each point in the Brillouin there is an associated field distribution and the result depends on the band considered. As the number of the band increases, the energy of the state also increases. The lower bands correspond to lower energies. The specific points for which the fields are calculated are those in the corners of the irreducible Brillouin zone (Points Γ, X, and M). In the Γ-point the value of the modulus of **k** is equal to zero, while in the X-point the modulus of the wave vector **k** is equal to π divided by the lattice constant a. This means that the wavelength of the electromagnetic wave at this point is twice the lattice constant a. This is an important point that helps to visualize the color maps. The same reasoning can be applied to the M-point. It is possible to obtain an idea of the energy of the mode by careful inspection of the field distribution. A basic fact that can be applied is the following: if the electric field is principally located in regions of high dielectric constant value, then the mode corresponds to the low energy band. Comparisons of different field distributions reveal relatively large energy differences among the modes. The colormaps are shown in the following pages.

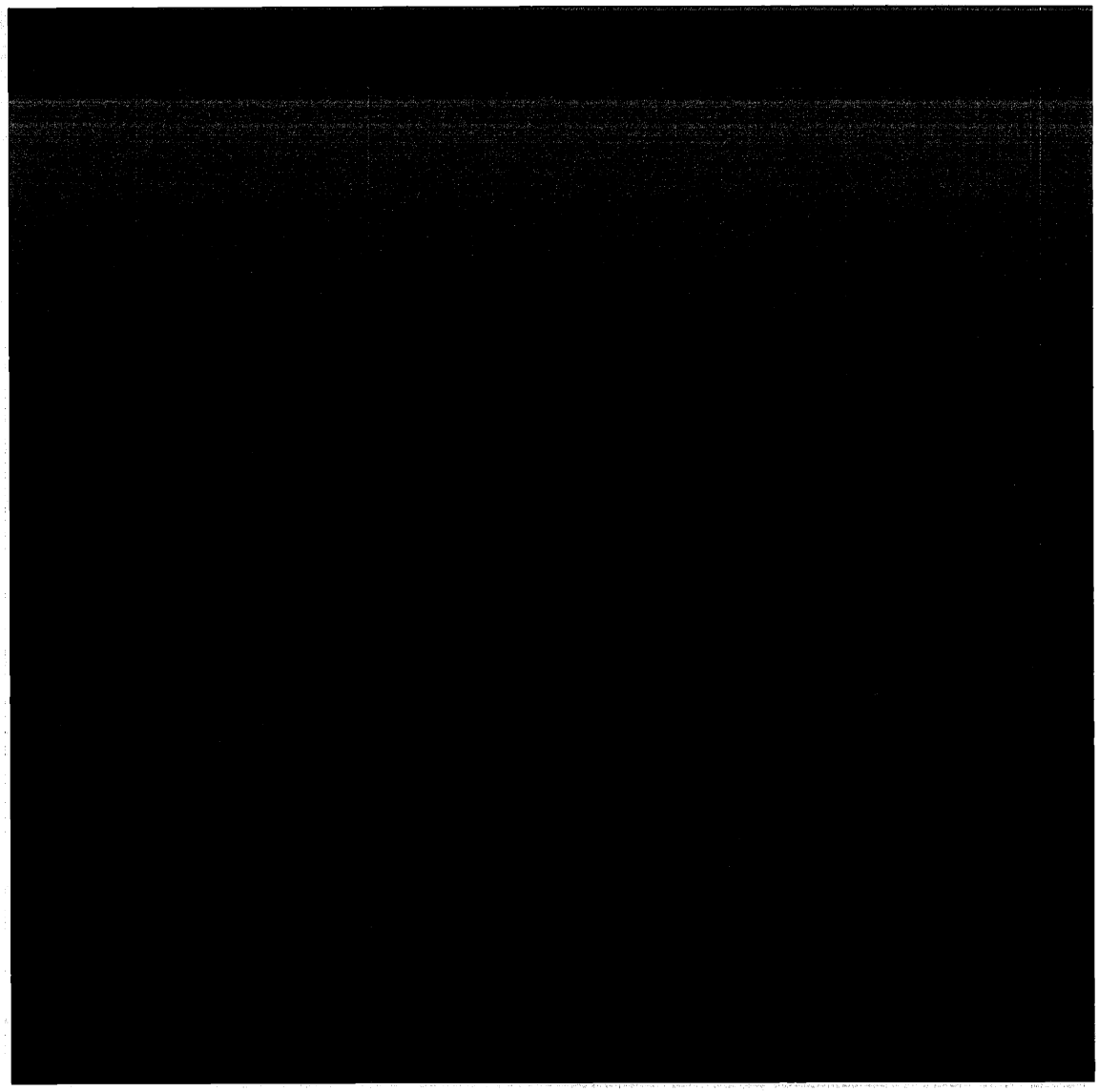

Fig. 4-5 Electric field distribution at Γ- point for TE polarization (1st band).

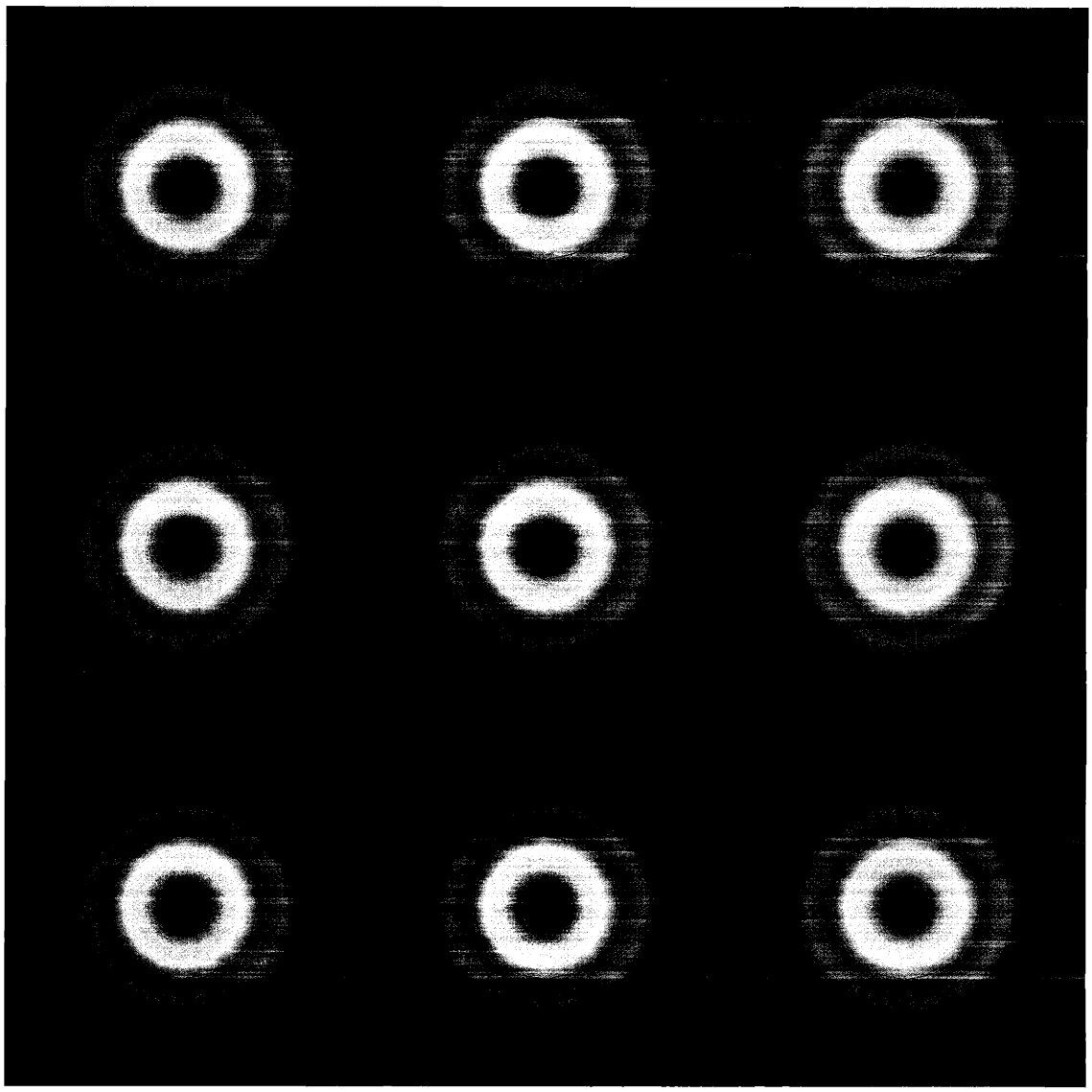

Fig. 4-6 Electric field distribution at Γ- point for TE polarization (2nd band).

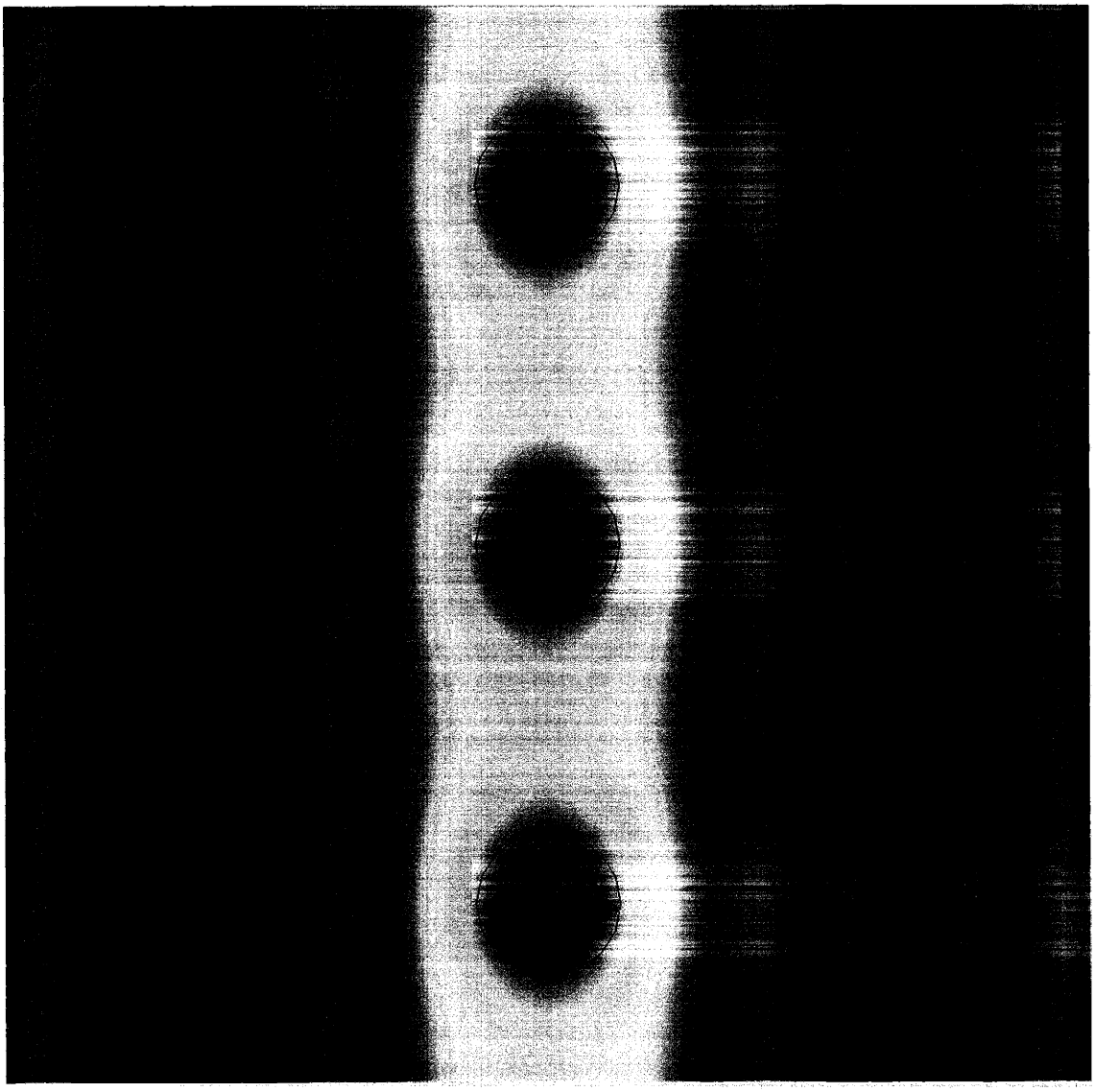

Fig. 4-7 Electric field distribution at X- point for TE polarization (1st band).

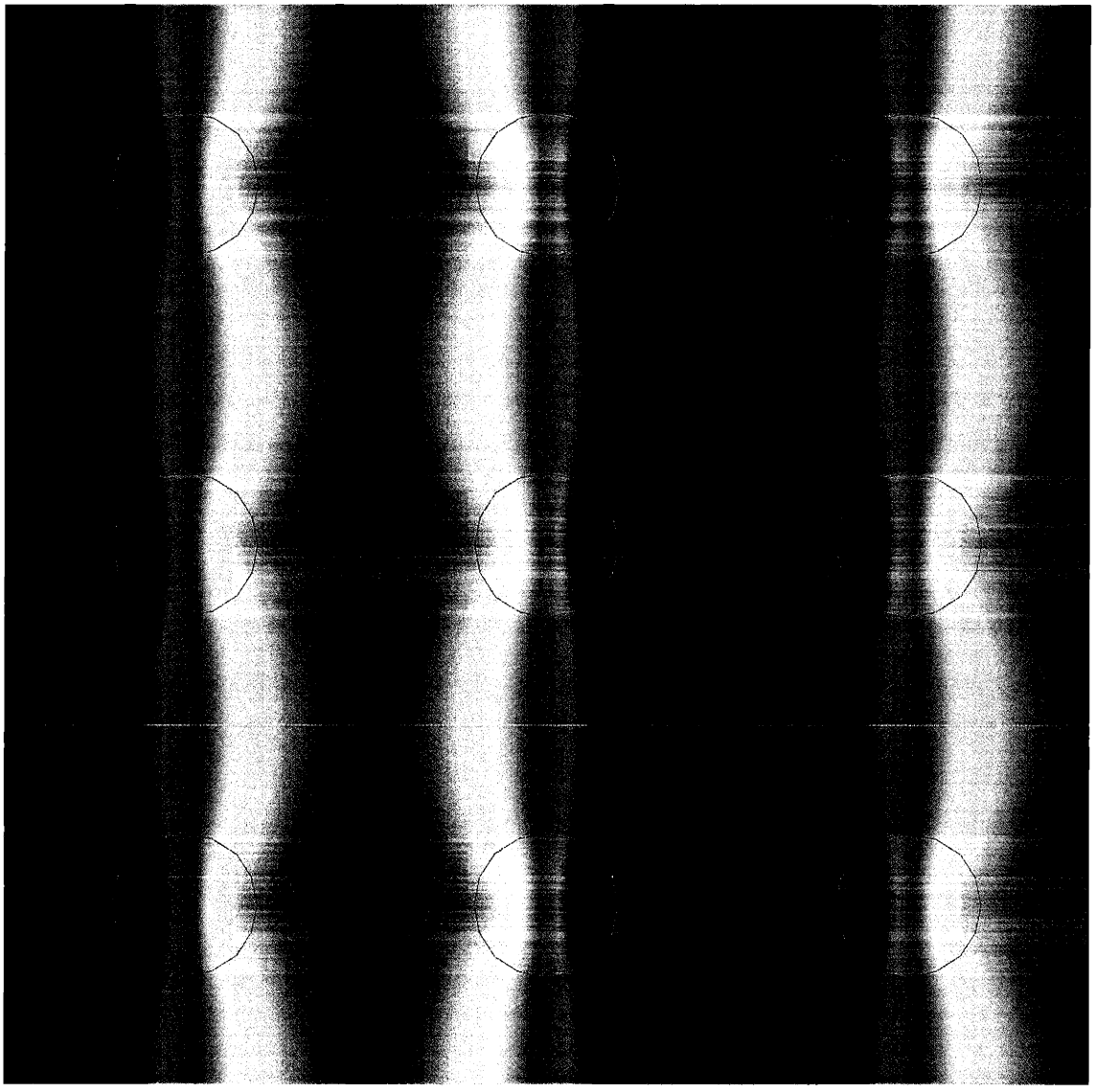

Fig. 4-8 Electric field distribution at X- point for TE polarization (2^{nd} band).

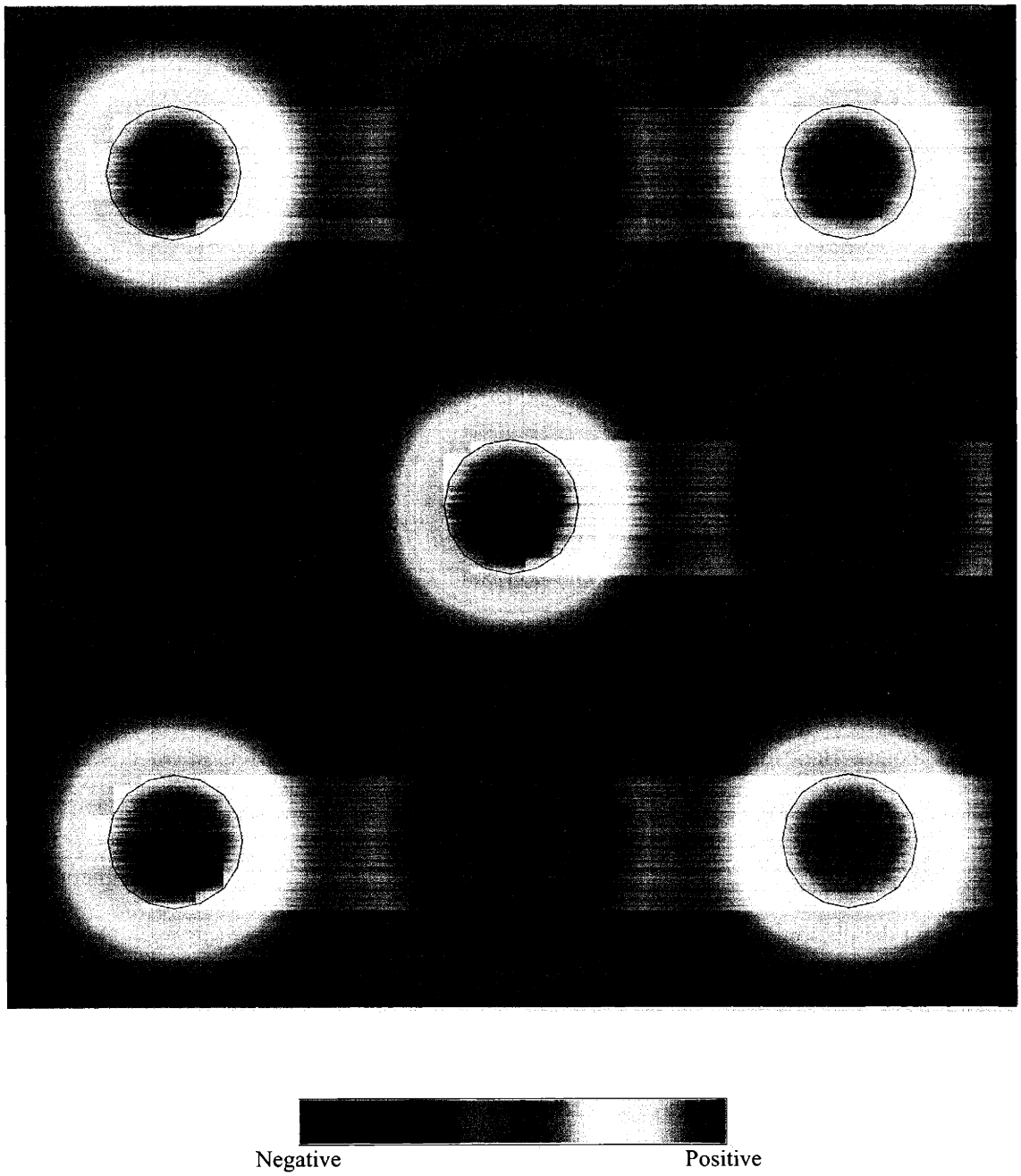

Fig. 4-9 Electric field distribution at M- point for TE polarization (1st band).

Chapter 5

Matrix Translation Method:

Reflectivity for 1-D photonic crystals

In Chapter 2 the differential equation for the magnetic field **H** of an electromagnetic wave traveling within isotropic, linear, and non-conducting media was derived from Maxwell's equations. Due to the assumption that the crystals hold infinite translational symmetry this equation became a standard eigenvalue problem in which the eigenvalue frequencies represent the allowed modes. Band diagrams could be found by using Fourier's Method. In this chapter a different formulation is used for studying one-dimensional photonic crystals. As a result, reflectance as a function of both the wavelength and the direction of the electromagnetic wave incident on the photonic crystal can be obtained. An important attribute of this method is that the photonic crystals are no longer considered to be infinite.

5.1 The Matrix Translation Method

In the Matrix Translation method, isotropic, linear, and non-conducting materials are considered. It is known that photonic crystals are made of different materials with different

dielectric constants. As a consequence, the dielectric constant of the structure changes with position. Matching conditions for the fields are needed at the interfaces between media.

Each Maxwell's interface condition is derived from one of Maxwell's equations using either Stoke's theorem or the divergence theorem. Stoke's theorem is used for equations involving curl operators and the divergence theorem is used for equations involving divergences operators. The Matrix Translation Method can be used to study omnidirectionality in multilayer films. Each film is considered composed of a homogeneous, isotropic, linear, and non-conducting medium. Furthermore, the relative magnetic permeability is equal to 1 for all media. The electromagnetic electric field can be written as

$$E_z^n(x,y) = (E_+^n e^{ik_{nx}x} + E_-^n e^{-ik_{nx}x}) e^{ik_y y} \quad , \quad k_{nx}^2 + k_y^2 = k_0^2 \varepsilon_{nr} \tag{5-1}$$

where n = number of layer, E_+^n , E_-^n = incident and reflected plane wave amplitudes for the electric field in layer n.

By applying the matching conditions, the fields in one layer can be related to the fields in the adjacent layer. By using a recurrence relationship, the fields in the first layer can be related to the fields in the last layer. This method can be extended to an arbitrary number of such layers by iteration. As a final result, reflectivity can be obtained for a arbitrary number of layers. A finite number of layers is considered in this case.

The photonic crystal is characterized by the thickness h_1, h_2 of the two alternating layers, the dielectric constants ε_1, ε_2, and the number of layers. The input parameters are the wavelength and direction of the electromagnetic wave incident on the first layer of the multilayer film. The output is the reflectivity of the multilayer film as a function of the wavelength for a given direction and polarization of the wave.

5.2 Reflectivity and omnidirectionality with the Matrix Translation Method

The following values for the thickness h_1, h_2 and the dielectric constants ε_1, ε_2 are chosen: h_1=0.8μm, h_2=1.65μm and ε_1=21.16, ε_2=2.56. These values are equal to those used in Chapter 3 where the Fourier's Method was used. This permits a comparison between the methods. For the calculations, a multilayer system composed of 14 layers was considered. The following graphs show reflectivity as a function of the wavelength of the incident wave. The first two graphs correspond to the results for normal incidence. One graph shows TE polarization and the other shows TM polarization. At normal incidence the results from these two graphs must be the same. When the value for reflectivity is equal to one, the wave cannot enter into the material and that particular wavelength (or frequency) is forbidden within the crystal. By making the change from wavelengths to frequencies, it can be seen that the values for which reflectivity is equal to one on the first two graphs (normal incidence) correspond to those forbidden frequency values in Fig 3-5 for the first gap. Agreement to within numerical accuracy is obtained between the Fourier's Method for an infinite system and the Matrix Translation Method for only 14 layers.

To find the omnidirectional gap using the results provided by the Matrix Translation Method, the following analysis is needed. Numerical examination of all angles of incidence for a given range of frequencies is required. By looking for the values of reflectivity equal to one, the omnidirectional gap can be obtained. The graphs in the following page show an omnidirectional gap in numerical agreement with the omnidirectional gap obtained by using the Fourier's Method.

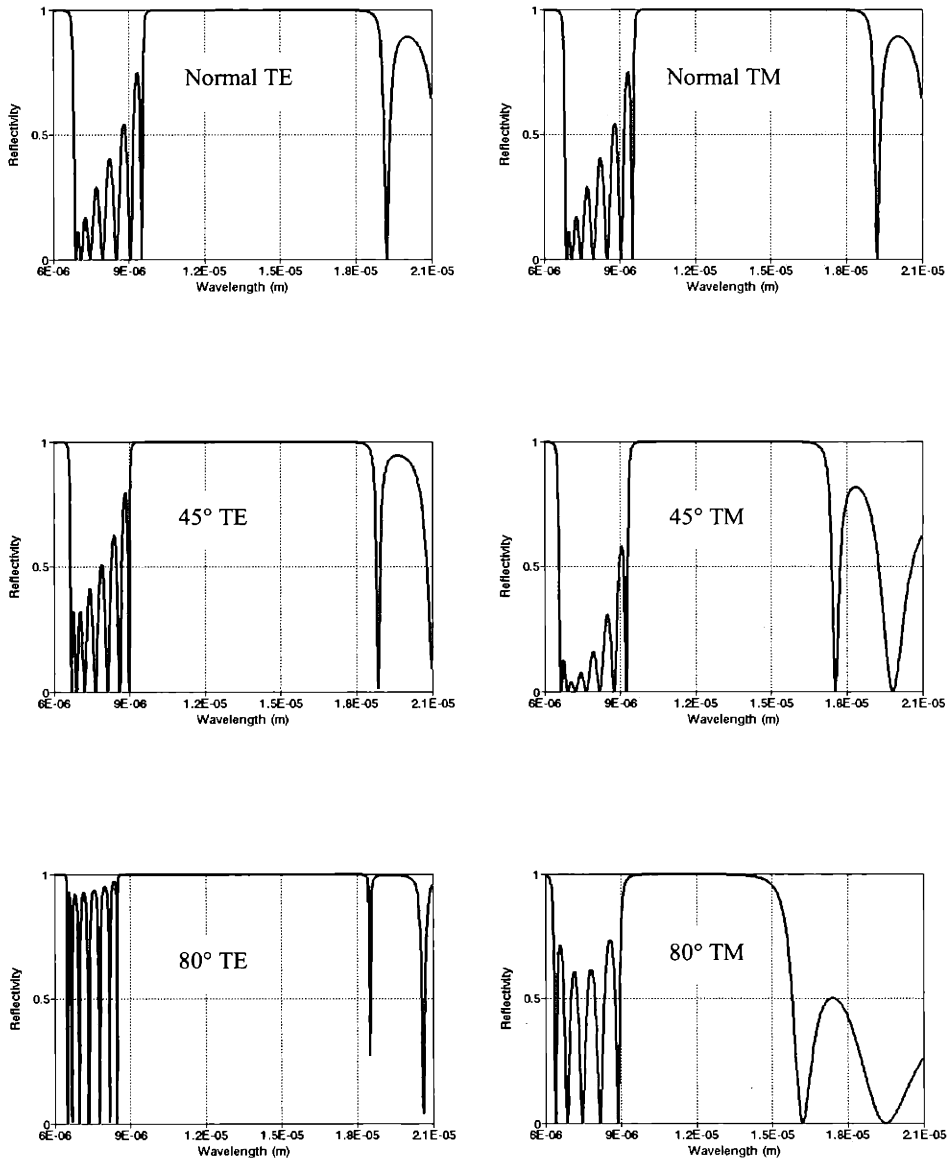

Fig. 5-1 Reflectivity as a function of the wavelength of the incident wave. Different directions and polarization are shown. The multilayer system consist of 14 layers of alternating media 1 and 2 with h_1=0.8μm, h_2=1.65μm and ε_1=21.16, ε_2=2.56.

Chapter 6

Conclusions

The new generation of photonic materials will require coordination between computational methods and experimental techniques for the development of novel material behavior. The solution of Maxwell's equations is absolutely necessary to gain an understanding of the physical processes that occur within the composite structure to predict and design photonic band gaps. The first assumption used in this thesis to describe them was to assume the materials to be infinite. With this assumption, Maxwell's equations were solved on a periodic domain which reduced the solution, via Bloch's theorem, to a standard eigenvalue problem. The problem is solved by a numerical algorithm for finding the correspondent eigenvalues. These mathematical eigenvalues are the allowed physical frequencies for a given direction of the wave vector of the incident planar wave. By searching for all the directions, the complete band structure could be obtained for given composite microstructures.

In the case of a particular 1-D system, a complete study of all allowed frequencies displays a resulting range of forbidden frequencies. In other words, for the detection of forbidden frequencies (photonic band gap), it was necessary to carry out a prior determination of all allowed frequencies. The numerical calculations showed for one-dimensional systems the existence of a complete gap for all directions for the particular photonic composite. The numerical simulation

predicts the existence of a material that acts as a perfect mirror in accordance with previous calculations and experiments.[10] Finally, because the scaling properties allow a normalization in a length and dielectric constant, generalized data for normal incidence can be efficiently compiled for a large number of photonic composites.

The two-dimensional system studied (an infinite square lattice of dielectric columns) did not produce a complete gap for all directions and polarizations. However, a photonic gap exists for TE polarization. The distributions of the fields (showed in color maps of intensity) gave an insight on the propagation of the wave within the photonic crystal. A complete study of these graphs can improve the understanding of the propagation of waves inside of photonic crystals.

In the case of one-dimensional systems, the assumption of infinite structure for the photonic crystal can be removed and a simple method for treating finite structures can be applied. The Matrix Translation Method proved to be an alternative for studying omnidirectional reflectivity. The method does not assume infinite structures and allows a study of photonic crystals with a finite number of layers. This formulation provides reflectivity as a function of the incident wavevector magnitude and directions and serves as a useful complement to band diagrams.

Suggestions for future work

- Application of Fourier's method to three-dimensional systems: More complicated geometries arise; as a consequence, efficient numerical algorithms are absolutely needed.
- Extension of the Matrix Translation Method to anisotropic systems and to include photonic losses in the material.
- Exploration of new methods for modeling photonic crystals such as the Finite Element Method or the Finite-Difference Time-Domain method.

References

1) J.D. Jackson, *Classical Electrodynamics*, 3rd Edition, New York: Wiley (1999).

2) J.R. Reitz, *Foundations of Electromagnetic Theory*, 4th Edition, Addison-Wesley (1993).

3) E. Yablonovitch, "Inhibited spontaneous emission in solid-state physics and electronics," *Phys. Rev. Lett.,* 58, 2059 (1987).

4) E. Yablonovitch and T.J. Gmitter, "Photonic band structure: The face-centered-cubic case," *Phys. Rev. Lett.,* 63, 1950 (1989).

5) M.A. Omar, *Elementary Solid State Physics*, Addison-Wesley (1993).

6) N.W. Ashcroft, *Solid State Physics*, Saunders College Publishing (1976).

7) K.M. Ho, C.T. Chan, and C.M. Soukoulis, "Existence of a photonic gap in periodic dielectric structures," *Phys. Rev. Lett.,* 65, 3152 (1990).

8) E. Yablonovitch, T.J. Gmitter, and K.M. Leung, "Photonic band structure: The face-centered-cubic case employing nonspherical atoms," *Phys. Rev. Lett.,* 67, 2295 (1991).

9) H.S. Sozuer, J.W. Haus, and R. Inguva, "Photonic bands: Convergence problems with the plane-wave method," *Phys. Rev. B,* 45, 13962 (1992).

10) Y. Fink, J.N. Winn, S. Fan, C. Chen, J. Michel, J.D. Joannopoulos, E.L. Thomas, "A Dielectric Omnidirectional Reflector," *Science*, Vol. 282, pp 1679-1682 (1998).

11) R.D. Meade, A.M. Rappe, K.D. Brommer, and J.D. Joannopoulos, "Accurate Theoretical Analysis of Photonic Band Gap Materials," *Phys. Rev. B*, 48, 8434, (1993).

12) J.D. Joannopoulos, *Photonic Crystals*, Princeton University Press (1995).